AP1 is essential for generation of autophagosomes from the trans-Golgi network

Yajuan Guo[1], Chunmei Chang[1], Rui Huang[1], Bo Liu[1], Lan Bao[2] and Wei Liu[1,*]

[1]Department of Biochemistry and Molecular Biology, Program in Molecular and Cell Biology, Zhejiang University School of Medicine, Hangzhou 310058, China
[2]Institute of Biochemistry and Cell Biology, Shanghai Institutes for Biological Sciences, Chinese Academy of Sciences, Shanghai 200031, China
*Author for correspondence (liuwei666@zju.edu.cn)

Accepted 17 November 2011
Journal of Cell Science 125, 1706–1715

doi: 10.1242/jcs.093203

Summary

Despite recent advances in understanding the functions of autophagy in developmental and pathological conditions, the underlying mechanism of where and how autophagosomal structures acquire membrane remains enigmatic. Here, we provide evidence that post-Golgi membrane traffic plays a crucial role in autophagosome formation. Increased secretion of constitutive cargo from the trans-Golgi network (TGN) to the plasma membrane induced the formation of microtubule-associated protein light chain 3 (LC3)-positive structures. At the early phase of autophagy, LC3 associated with and then budded off from a distinct TGN domain without constitutive TGN-to-plasma cargo and TGN-to-endosome proteins. The clathrin adaptor protein AP1 and clathrin localized to starvation- and rapamycin-induced autophagosomes. Dysfunction of the AP1-dependent clathrin coating at the TGN but not at the plasma membrane prevented autophagosome formation. Our results thus suggest an essential role of the TGN in autophagosome biogenesis, providing membrane to autophagosomes through an AP1-dependent pathway.

Key words: AP1, LC3, Autophagosome, Membrane trafficking, Trans-Golgi network

Introduction

Autophagy is a highly conserved process in eukaryotic cells and is a mechanism for the turnover of cytoplasmic materials in a lysosome-dependent pathway. It is used either to provide nutrients during starvation or as a quality control that eliminates obsolete macromolecules and organelles during cell growth. In addition to the identification of more than 30 autophagy-related genes (Atgs) whose products are required for autophagic vacuole formation and development, recent studies have revealed that autophagy is involved in multiple physiological and pathological processes, including immunity, aging, neurodegenerative diseases and tumorigenesis.

Despite the progress achieved in understanding the molecular basis of autophagy and its important role in physiological and pathological situations, two crucial issues remain unclear: the origin of the smooth membrane cisternae, and the mechanism by which autophagosomal structures acquire membrane. To date, extensive evidence suggests that the autophagic membranes are derived from pre-existing cytoplasmic membrane compartments including the endoplasmic reticulum (ER), the Golgi complex and mitochondria (Juhasz and Neufeld, 2006; Reggiori and Tooze, 2009). Because it is the largest intracellular membrane source in eukaryotic cells, the ER appears to be the origin of autophagosomal membrane based on the discovery of ER marker enzymes in pre-autophagosomal structures (Arstila and Trump, 1968; Ericsson, 1969). In addition, it has been found that phosphatidylinositol 3-phosphate [PtdIns(3)*P*]-enriched membranes dynamically connect to the ER and provide a membrane platform for autophagosomes (Axe et al., 2008). Recently, this physical connection between the ER and autophagosomes has been confirmed by 3D electron tomography (Hayashi-Nishino et al., 2009; Yla-Anttila et al., 2009). Based on these observations, it has been proposed that a portion of the ER is cleared of ribosomes and folds onto itself to form the isolation membrane (IM), which is a forming autophagosome cradled between two ER membranes (Axe et al., 2008; Hayashi-Nishino et al., 2009).

However, many studies have also reported that some Atg proteins essential for autophagosome formation act at sites outside the ER. Beclin1, the mammalian homolog of yeast Atg6, which is important in mediating the localization of other autophagy proteins to pre-autophagosomal structures, functions mainly at the trans-Golgi network (TGN) as part of a class III PI3K complex (Kihara et al., 2001). The sole transmembrane Atg protein, Atg9, is located in the TGN and travels between the TGN and endosomes in mammalian cells (Young et al., 2006). The Golgi-resident small GTPase, Rab33B, interacts with Atg16L and modulates autophagosome formation (Itoh et al., 2008). In yeast, subunits of the conserved oligomeric Golgi complex localize to the phagophore assembly site and are required for the formation of double-membrane cytoplasm-to-vacuole targeting vesicles and autophagosomes (Yen et al., 2010). All these observations highlight the importance of the Golgi complex, including the TGN, in the biogenesis of autophagosomes. In addition to its localization in the TGN, Atg9 in yeast also targets to mitochondria and travels between mitochondria and the pre-autophagosomal structure (PAS) (Reggiori et al., 2005). In mammalian cells, Atg5 and microtubule-associated light chain 3 (LC3) transiently localize to punctae on mitochondria, and the tail-anchor of a mitochondrial outer membrane protein also labels autophagosome membranes and is sufficient to deliver another

Journal of Cell Science

outer mitochondrial membrane protein to autophagosomes (Hailey et al., 2010). These data indicate a connection between mitochondria and autophagosomal structures, and confirm that mitochondria contribute membrane to autophagosomes. More recently, it has been reported in mammalian cells that the coat protein clathrin interacts with Atg16L and is required for the formation of Atg16L-positive autophagosome precursors from the plasma membrane by endocytosis, suggesting that the plasma membrane is a membrane reservoir for inducible autophagosome formation (Ravikumar et al. 2010).

LC3 is the first protein shown to specifically label autophagosomal membranes in mammalian cells (Kabeya et al., 2000) and it is involved in both the origin and elongation of the autophagosomal membranes. Association of LC3 with autophagosomal membranes requires relocation of the protein from the nucleus (Darke et al., 2010), several steps of post-translational modification of pro-LC3, including cleavage at its C-terminal G120 site to form a soluble LC3-I, and a subsequent attachment of phosphatidylethanolamine (PE) to form membrane-bound LC3-II (Tanida et al., 2004; Sou et al., 2006). In this study, using LC3-II as an autophagosomal membrane marker, we investigated the regulatory function of intracellular membrane trafficking in autophagosome formation by modulating the protein secretory pathway at different steps in mammalian cells. We showed that a transient increase in constitutive cargo flow from the TGN to the plasma membrane initiates the generation of LC3-positive vesicles. Blockage of post-Golgi transport, by disrupting AP1-dependent clathrin coating in the TGN, inhibited autophagy. We also showed association of LC3 with the TGN, and AP1 and clathrin with autophagosomes, during autophagy. Our observations suggest a crucial contribution of TGN membrane and AP1 and clathrin coats to autophagosome formation.

Results

ER export is essential for autophagosome formation

To investigate a possible regulatory effect of the secretory pathway on autophagy in mammalian cells, we assessed the effect of disrupting ER–Golgi trafficking by overexpression of different mutants that interfere with the core functions of the small GTPases Sar1 and Arf1 in the formation of COPII and COPI vesicles (Pucadyil and Schmid, 2009). In HEK293 cells expressing green fluorescent protein (GFP)-tagged LC3, one hour of starvation triggered a dramatic increase in the generation of autophagosomes in the cytoplasm, indicated as GFP–LC3-positive spot-like structures (Fig. 1A). Transient expression of human influenza hemagglutinin (HA)-tagged Arf1T31N, a constitutively inactive Arf1 (Dascher and Balch, 1994; Klausner et al., 1992), Sar1T39N, a constitutively inactive Sar1 (Barlowe et al., 1994; Kuge et al., 1994; Shima et al., 1998) or Sar1H79G, a constitutively active Sar1 (Aridor et al., 1995), prevented starvation-induced autophagosome formation (Fig. 1A,B). Because the amount of LC3-II represents membrane-bound LC3 and the level of autophagy (Kabeya et al., 2000), we measured by western blot the level of LC3-II during starvation with or without the lysosome inhibitor bafilomycin A1 (BafA1). As a result, transiently expressed Arf1T31N–HA significantly suppressed the starvation- and BafA1-induced elevation of LC3-II (Fig. 1C). These data are consistent with previous observations in yeast (Hamasaki et al., 2003) and suggest that the secretory pathway is essential to autophagosome formation in mammalian cells.

Increased TGN-to-plasma traffic stimulates the formation of LC3-vesicles

To test whether increased secretory traffic affects the formation of autophagosomes, we visualized the change in intracellular localization of GFP–LC3 during release of a bolus of the thermo-reversible folding mutant, ts045 vesicular stomatitis virus G protein fused to fluorescent protein Cherry at its cytoplasmic tail (VSVG–Cherry), from the ER into the secretory pathway by shifting the temperature from 40℃ to 32℃ (Bergmann, 1989; Presley et al., 1997). There were no dramatic changes in GFP–LC3 distribution when VSVG–Cherry was localized in the ER at 40℃ or reached the juxtanuclear Golgi complex within 40 minutes after changing the temperature (Fig. 2A). Unexpectedly, in ~45% of cells expressing VSVG–Cherry and GFP–LC3, by 120 minutes

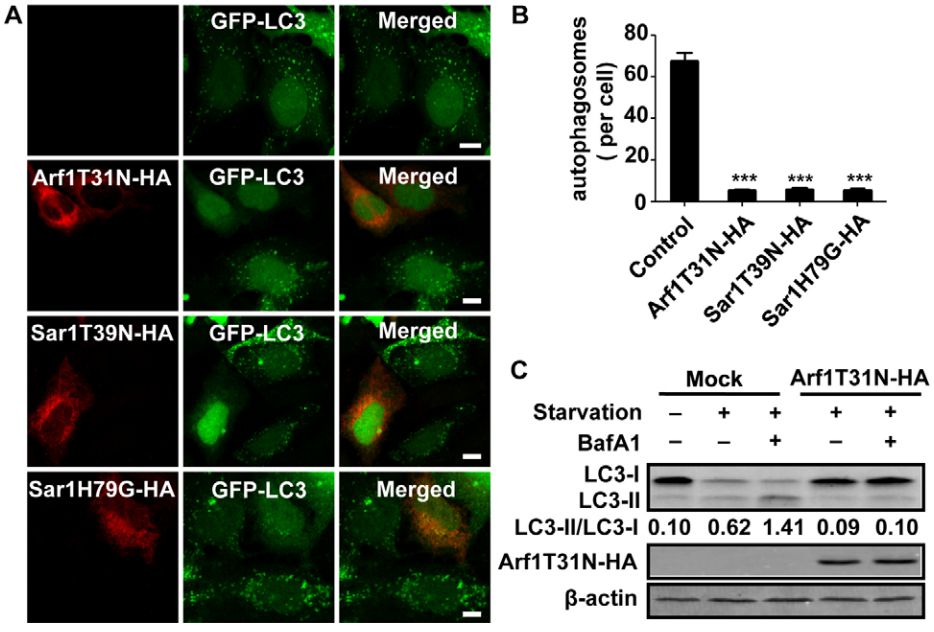

Fig. 1. The early secretory pathway is essential for autophasome formation. (**A**) HEK293 cells transiently expressing GFP–LC3 or GFP–LC3 and HA-tagged Arf1 or Sar1 mutants, were incubated in starvation medium for 1 hour and imaged by confocal microscopy. Scale bars: 10 μm. (**B**) Statistical analysis of the numbers of LC3 dots per cell in A. Quantification of autophagosomes per cell was done using the Axiovision automatic measurement program on the Zeiss LSM510 Meta as described in the Materials and Methods. The values reported are means ± s.e.m.; ***P<0.0001 vs control. (**C**) HEK293 cells with or without Arf1T31N–HA expression were cultured in starvation medium with or without BafA1 for 1 hour; the cellular LC3 level was assessed by western blot. The LC3-II to LC3-I ratio was evaluated by densitometric analysis.

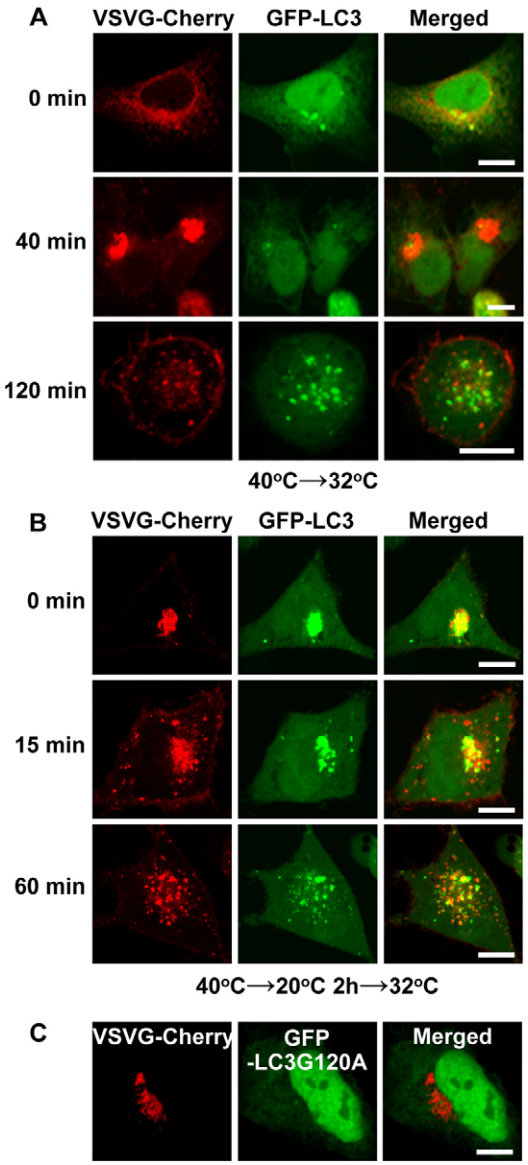

Fig. 2. Enhanced TGN-to-PM transport stimulates autophagosome formation. (**A**) HEK293 cells transiently expressing GFP–LC3 and VSVG–Cherry were incubated at 40℃ overnight to retain VSVG–Cherry in the ER. Then the cells were imaged over time upon shifting the culture temperature from 40℃ to 32℃. (**B**) HEK293 cells expressing GFP–LC3 and VSVG–Cherry were incubated at 40℃ overnight, followed by culture for 2 hours at 20℃ to retain VSVG–Cherry in the TGN. Then the culture temperature was shifted to 32℃, and the cells were imaged at indicated time points after the temperature shift. (**C**) HEK293 cells expressing GFP–LC3G120A and VSVG–Cherry were incubated at 40℃ overnight, followed by 2 hours culture at 20℃ to retain VSVG–Cherry in the TGN and imaged. All fluorescence images were confocal images of optical slice thickness ~1 μm. Scale bars: 10 μm.

after the temperature shift, when a large amount of the VSVG–Cherry left the Golgi complex and arrived at the plasma membrane, a large number of spot-like GFP–LC3-positive structures appeared in the cytoplasm, representing increased autophagic vesicles (Fig. 2A). This observation implies that increased Golgi-to-plasma-membrane (PM) traffic promotes the basal level of autophagosomes.

To confirm that the Golgi-to-PM transport in the secretory pathway enhances autophagosome formation, we designed another experiment by shifting the culture temperature of HEK293 cells expressing GFP–LC3 and VSVG–Cherry from 40℃ to 20℃ for 2 hours to directly accumulate VSVG–Cherry in the TGN, then changing the temperature to 32℃, allowing the cargo to go to the PM (Griffiths et al., 1985; Matlin and Simons, 1983). Surprisingly, at 20℃, in ~80% of the cells, GFP–LC3 was found to strongly associate with the TGN as demonstrated by colocalization of GFP–LC3 with VSVG–Cherry in the perinuclear region (Fig. 2B). Changing the temperature from 20℃ to 32℃ for 15 minutes, when part of the VSVG–Cherry left the TGN for the plasma membrane, the GFP–LC3 started to bud off from the TGN separate from the VSVG–Cherry. After changing the temperature for 60 minutes, when more VSVG–Cherry left the TGN, GFP–LC3 dispersed into small-spot structures, which morphologically resembled autophagosomes (Fig. 2B).

To determine the specificity of the association of GFP–LC3 with the TGN, we introduced a mutation changing the Gly120 to Ala (LC3G120A) in LC3, which affects the cleavage at the C-terminal region of pro-LC3 and results in failure to form LC3-I and LC3-II (Kabeya et al., 2000). When expressed in the cells with VSVG–Cherry, GFP–LC3G120A never bound to the TGN with the same loading of VSVG–Cherry onto the TGN by shifting the temperature from 40℃ to 20℃ for 2 hours (Fig. 2C). This result strongly suggests that binding of LC3 to the TGN is mediated by a specific interaction between LC3 and the TGN membrane, and TGN-associated LC3 is the membrane-bound LC3–PE.

To exclude the possibility that these events were purely a result of temperature change, we performed the same experiments in cells expressing LC3–GFP only or LC3–GFP with pmCherry-C1. The results showed that the temperature change itself did not stimulate the membrane association of LC3 and the subsequent production of LC3-positive vesicles in any of the cells (supplementary material Fig. S1).

Blockade of post-Golgi transport prevents starvation- or rapamycin-induced autophagosome formation

To obtain further evidence that TGN-to-PM traffic regulates autophagosome formation, we then assessed the generation of autophagosomes when TGN-to-PM transport was blocked. Clathrin adaptor protein 180 (AP180) and EGFR pathway substrate clone 15 (Eps15) mediate the formation of TGN-derived vesicles. Overexpression of an AP180 C-terminal domain (AP180C, residues 530–915) or an Eps15 deletion mutant lacking the second and third N-terminal EH domains (Eps15Δ95/295) has a dominant-negative effect on clathrin coating at the TGN (Chi et al., 2008; Zhao et al., 2001). When expressed in cells, AP180C–YFP and YFP–Eps15Δ95/295 almost fully prevented the transport of VSVG–CFP from the TGN to the PM (Fig. 3A) (Chi et al., 2008). In these cells, induction of autophagosome-like vesicles by releasing VSVG–CFP from TGN-to-PM transport was also diminished, although Cherry–LC3 was still recruited to the TGN by VSVG loading (Fig. 3B,C). The effect of AP180C–YFP and YFP–Eps15Δ95/295 expression was also determined in autophagosome formation induced by starvation. Starvation that induced typical autophagy in control cells resulted in fewer autophagosomes in cells expressing AP180C–YFP or YFP–Eps15Δ95/295 (Fig. 3D,F), suggesting a fundamental role of exit from the TGN in the regulation of autophagosome biogenesis.

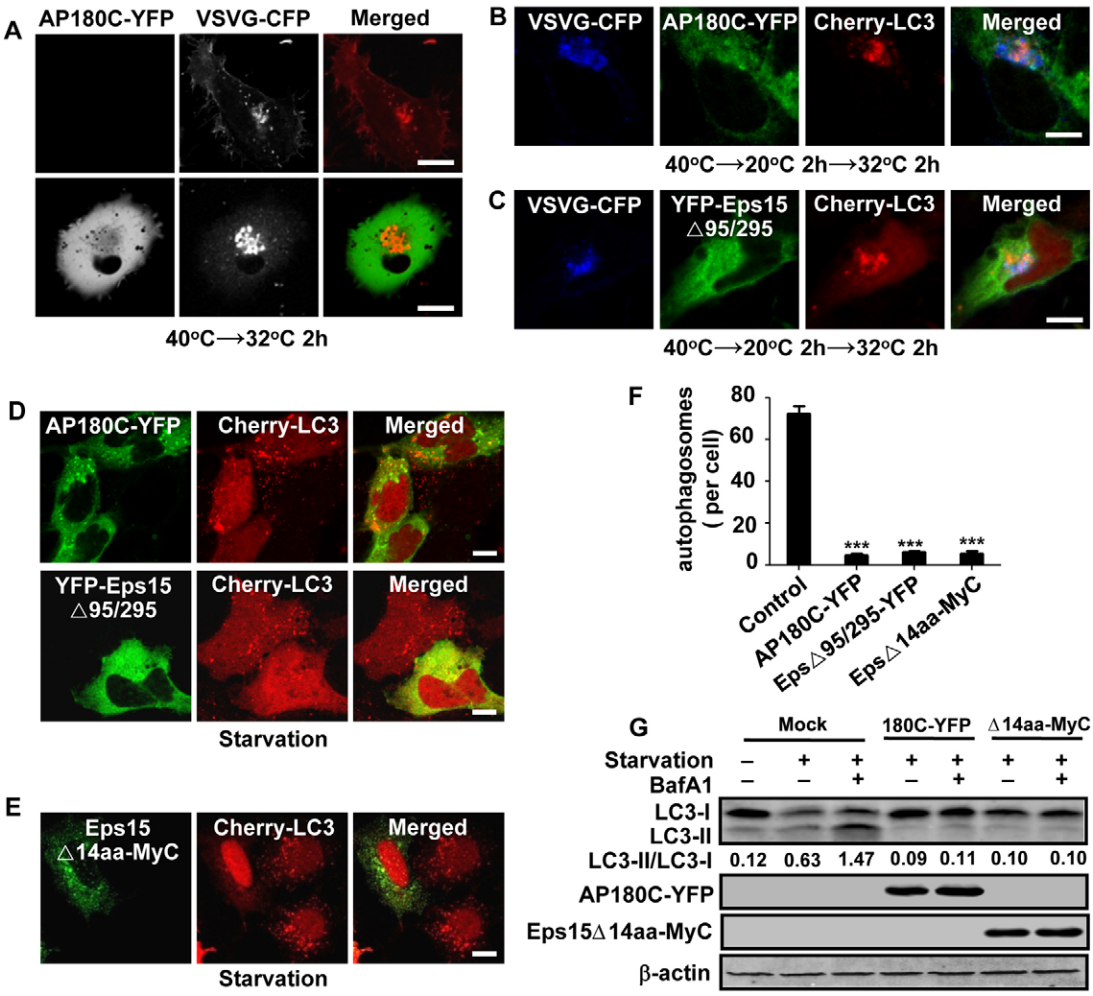

Fig. 3. Blockade of TGN-to-PM transport inhibits autophagosome formation. (**A**) HEK293 cells expressing VSVG-CFP with or without AP180C–YFP were incubated at 40℃ for 15 hours. Then the cells were shifted to 32℃ for 2 hours and imaged. (**B**,**C**) Cells expressing VSVG–CFP and Cherry–LC3 with AP180C–YFP (B) or YFP–Eps15Δ95/295 (C) were incubated at 40℃ for 15 hours and at 20℃ for 2 hours. Then the cells were shifted to 32℃ for 2 hours and imaged. Note the retention of VSVG–CFP and Cherry–LC3 in the TGN. (**D**,**E**) HEK293 cells expressing Cherry–LC3 with or without AP180C–YFP or YFP–Eps15Δ95/295 (D), or Eps15Δ14aa-MyC (E), were cultured in starvation medium for 1 hour. Then the cells were either directly imaged (D) or were fixed, followed by immunofluorescence staining with anti-Myc antibody and Alexa-Fluor-488-tagged secondary antibody (E). All fluorescence images were confocal images of optical slice thickness ~1 μm. Scale bars: 10 μm. (**F**) Statistical analysis of the numbers of LC3 dots per cell in D and E. Quantification of autophagosomes per cell was done using the Axiovision automatic measurement program on the Zeiss LSM510 Meta as described in the Materials and Methods. The values reported are means ± s.e.m.; ***$P<0.0001$ vs control cells. (**G**) HEK293 cells were transiently transfected with or without AP180C–YFP or Eps15Δ14aa–Myc. Cells were starved for 1 hour with or without BafA1, and analyzed by western blot. The LC3-II to LC3-I ratio was evaluated by densitometric analysis.

AP180C or Eps15Δ95/295 removes clathrin from not only the TGN but also the PM (Benmerah et al., 1998; Ford et al., 2001; Lui-Roberts et al., 2005). To ensure that the observed reduction of autophagosomes in AP180 and Eps15 mutant cells was a direct effect on the TGN and did not result from disruption of endocytosis, we used another mutant Eps15 protein, which lacked a 14 amino acid motif (Eps15Δ14aa). Expression of Eps15Δ14aa selectively reduces the exit of secretory proteins from the TGN by binding to AP1, but not AP2 (Chi et al., 2008). We found that expression of Eps15Δ14aa–MYC also dramatically suppressed starvation-induced autophagosome formation in HEK293 cells (Fig. 3E,F).

Finally, we measured the LC3–PE level in cells overexpressing AP180 or Eps15 deletion mutants by western blot. As expected, the starvation- and BafA1-induced elevation in LC3–PE level was clearly suppressed (Fig. 3G), indicating that autophagosomes failed to form in these mutant cells. Collectively, these data suggest that not only the constitutive TGN-to-PM traffic but also general transport from the TGN is required for the formation of autophagosomes.

AP1 localizes to starvation- and rapamycin-induced autophagosomes

Our results showing that AP180 and Eps15 mutants disrupted the formation of LC3-posive vesicles from the TGN strongly suggested a requirement for a clathrin coat in the process. Because recruitment of clathrin to the TGN is mainly mediated by its adaptor protein AP1, it can assemble into a coat lattice, therefore we checked the distribution of AP1 during autophagy. HEK293 cells were transiently transfected with GFP-tagged

γ-adaptin (a subunit of the AP1 complex) and Cherry–LC3. In these cells, γ-adaptin–GFP presented a typical cytosol and TGN localization. Surprisingly, upon starvation for 1 hour or rapamycin treatment for 20 hours, in ~30% of cells, γ-adaptin–GFP redistributed to the formed autophagosomes showing a perfect colocalization with membrane-bound Cherry–LC3. In these cells, nearly every autophagosome contained γ-adaptin–GFP (Fig. 4A).

Previous studies have shown that Atg9 localizes to the TGN and cycles between the TGN and its peripheral pool during autophagy (Young et al., 2006). To further determine the action of AP1, especially in the early stage of autophagy, we expressed γ-adaptin–GFP and Cherry–Atg9 in the cells and analyzed their distribution during starvation or rapamycin treatment. At a very early phase of starvation (20 minutes) or rapamycin treatment (10 hours), colocalization of γ-adaptin–GFP and Cherry–Atg9 was detected (Fig. 4B). The specificity of AP1–LC3 and AP1–Atg9 colocalization was verified by visualizing GFP–α-adaptin (a subunit of the AP2 complex) with Cherry–LC3 and GFP–α-adaptin with Cherry–Atg9. As a result, neither starvation nor rapamycin treatment caused colocalization of AP2 with LC3 or Atg9 in any of the cells (supplementary material Fig. S2).

We also analyzed the colocalization of LC3 with clathrin during starvation. In GFP–LC3-expressing HEK293 cells, after starvation, the cells were stained with a specific anti-clathrin heavy-chain antibody. We found that in some cells (~30%), clathrin also distributed to the GFP–LC3-positive autophagosomes (Fig. 4C). These data thereby strongly suggested an involvement of AP1 and the clathrin coat in the formation of autophagosomes.

Because the colocalization of AP1 or clathrin with GFP–LC3-positive autophagosomes was only found in ~30% of cells, we then tested whether the remaining LC3-positive structures colocalized with other membrane organelles such as ER or mitochondria. Using a YFP-tagged mitochondrial matrix protein as a marker for mitochondria and a GFP-tagged KDEL receptor for the ER, we found that during starvation, Cherry–LC3 rarely colocalized with these markers (supplementary material Fig. S3).

LC3 binds to the TGN and forms LC3 vesicles from the TGN during starvation-induced autophagy

We next asked whether we could detect the outgrowth of similar vesicles from the TGN membrane in response to starvation. In fact, in cells overexpressing LC3, we often found high LC3 signals in the peri-nuclear region during autophagy. We therefore chose to stain starved HEK293 cells with antibodies against LC3 and TGN46 to check the intracellular localization of these endogenous proteins. We found that as early as 15 minutes of starvation, endogenous LC3 accumulated in peri-nuclear TGN46-positive sites (Fig. 5A). Nevertheless, LC3 was segregated from TGN46, suggesting it is associated with a unique non-TGN46-containing TGN sub-compartment. Over 30 minutes of starvation, the LC3 started to disperse from the TGN area and distribute randomly in the cytoplasm (Fig. 5A).

To determine the localization of LC3 on the TGN more precisely, we took a series of images through the Z-axis of cells stained with antibodies against LC3 and TGN46. The stacks were reconstructed to create 3D images. A typical 3D image of a cell starved for 20 minutes showed that on the TGN, most of the LC3 did not fuse with TGN46 (Fig. 5B), confirming that LC3 was associated with a non-TGN46-containing sub-compartment of the TGN membrane.

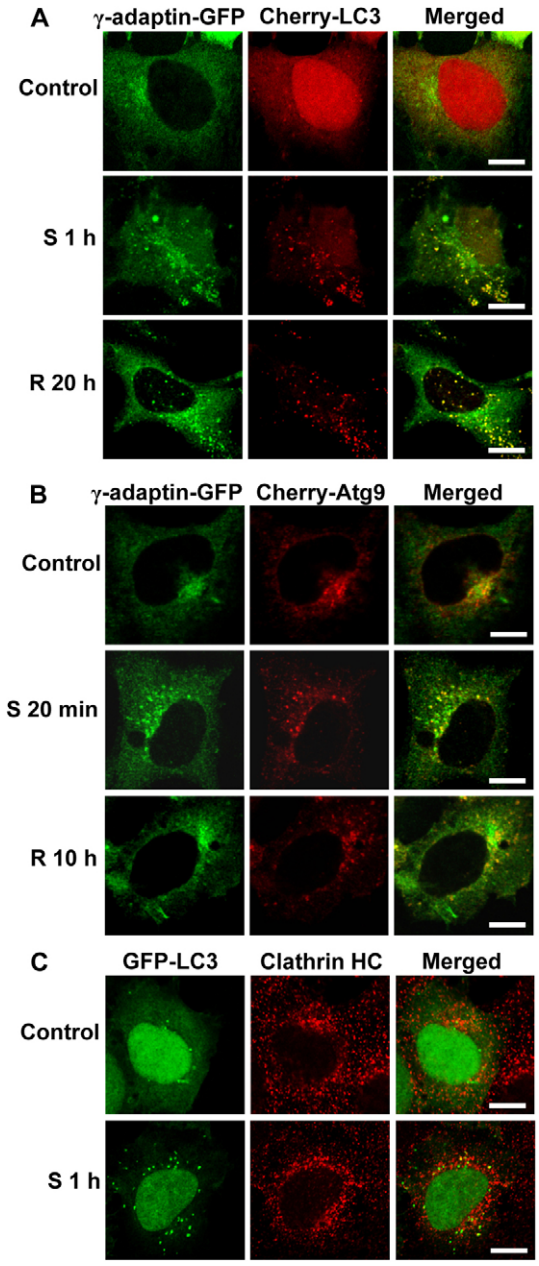

Fig. 4. Localization of AP1 to autophagosomes. (**A**) HEK293 cells expressing γ-adaptin–GFP and Cherry–LC3 were imaged after incubation in starvation medium for 1 hour or treatment with rapamycin for 20 hours. Note the colocalization of γ-adaptin–GFP with autophagosomes. (**B**) HEK293 cells expressing γ-adaptin–GFP and Cherry–Atg9 were imaged after incubation in starvation medium for 20 minutes or treatment with rapamycin for 10 hours. (**C**) HEK293 cells expressing GFP–LC3 were left untreated or starved for 1 hour. Then the cells were fixed and stained with antibody against clathrin heavy chain and Alexa-Fluor-545-tagged secondary antibody. All fluorescence images were confocal images of optical slice thickness ~1 μm. Scale bars: 10 μm. S, starvation; R, rapamycin.

We further visualized the budding process of GFP–LC3 from the TGN during starvation-induced autophagy in living cells. We found in some cells that GFP–LC3-containing membrane pulled off from the TGN as tubular processes that extended for several micrometers (supplementary material Fig. S4). GFP–LC3

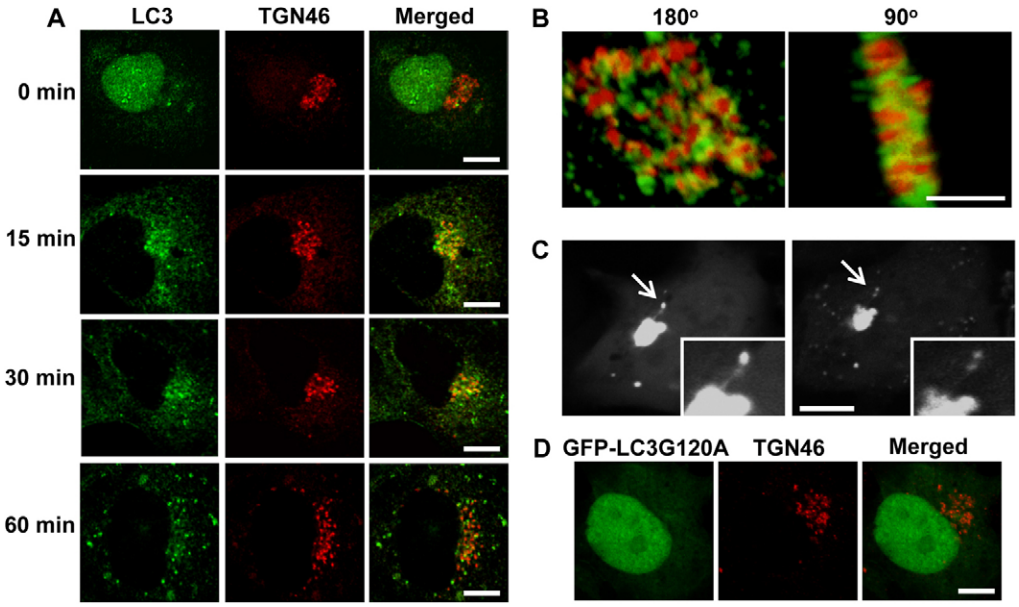

Fig. 5. TGN association with LC3 and formation of LC3-containing vesicles. (**A**) Dynamics of LC3 distribution during starvation. HEK293 cells cultured in starvation medium were fixed at indicated time points, stained with antibodies against LC3 and TGN46, followed by Alexa-Fluor-488- and Alexa-Fluor-545-tagged secondary antibodies. Then the cells were imaged by confocal microscopy. Scale bars: 10 μm. (**B**) 3D image of TGN-associated LC3. HEK293 cells cultured in starvation medium for 20 minutes were fixed, followed by immunofluorescence staining for LC3 and TGN46. A total of 39 images through the *Z*-axis of a cell were taken at 0.1 μm intervals, and the image stacks were reconstructed to 3D images. Shown are orthogonal sections of 180° and 90° of a single cell. Scale bar: 5 μm. (**C**) Live-cell imaging of TGN-associated GFP–LC3 in starved HEK293 cells. Note the formation of tubular structures from the TGN. Inset shows a magnification of region indicated by arrow. Scale bar: 10 μm. (**D**) HEK293 cells expressing GFP–LC3G120A were starved for 30 minutes and fixed, followed by immunofluorescence staining with anti-TGN46 antibody and Alexa-Fluor-545-tagged secondary antibody. Scale bar: 10 μm.

accumulated at the tips of these tubules, where they formed a ball-like mass. After a variable time, the tip regions detached and moved outward as separate elements. Sometimes during the detachment, the tip region was further divided into two vesicles (Fig. 5C).

We performed the same experiments to observe the dynamics of the GFP–LC3G120A mutant during starvation. We found, similar to VSVG loading (Fig. 2C), starvation never recruited the GFP–LC3G120A to the peri-nuclear region (Fig. 5D), further confirming a specific interaction of LC3–PE and the TGN membrane. Taken together, these data suggest that the TGN membrane is a source of membrane for autophagosomal structures.

Separation of LC3-containing vesicles from TGN-to-endosome traffic

Once formed, autophagosomes are required to fuse with the endosomal compartments and further fuse with lysosomes for maturation. Although the role of the endosomal system in autophagosome formation remains to be understood, results from yeast studies indicate that endosomes might not be essential for autophagosome assembly (Reggiori et al., 2004). The observation that LC3-positive vesicles bud off from a distinct domain of the TGN and remain separated from the constitutive cargos (VSVG) prompted us to clarify whether this occurs in TGN-to-endosome transport. We first observed the location of TGN38 (rat homolog of human TGN46) during autophagosome formation triggered by enhanced TGN-to-PM transport. In cells expressing both CFP–TGN38 and Cherry–LC3, on release of a bolus of VSVG–YFP from the TGN to the PM, very little CFP–TGN38 was found to localize to the LC3-positive vesicles derived from the TGN (Fig. 6A). We also did a time-course study with higher resolution imaging to observe the location of YFP–LC3 and endogenous

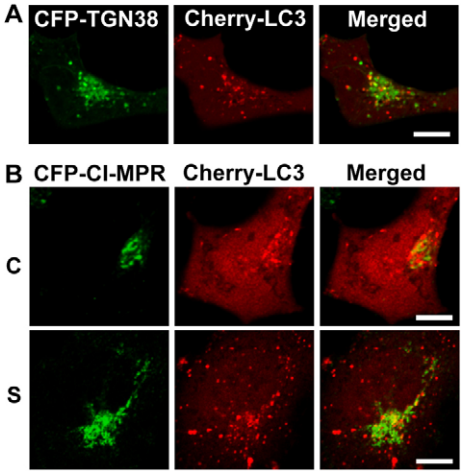

Fig. 6. Segregation of LC3 from components of TGN-to-endosome trafficking. (**A**) HEK293 cells transiently expressing Cherry–LC3 and CFP–TGN38 together with VSVG-YFP were cultured at 40℃ shortly after transfection to retain VSVG–YFP in the ER. Then the cells were incubated at 20℃ for 2 hours to accumulate VSVG–YFP in the TGN. Cells were imaged over time after shifting from 20℃ to 32℃. Shown are the distributions of LC3–Cherry and CFP–TGN38 at 60 minutes after the shift. (**B**) HEK293 cells transiently expressing LC3–Cherry and CFP-CI-MRP were left untreated or starved for 1 hour and imaged by confocal microscopy. C, control; S, starvation. Scale bars: 10 μm.

TGN46 during release of VSVG–CFP from the TGN. We found that, similar to the observations in starved cells, YFP–LC3 on the TGN caused by VSVG–CFP loading was initially segregated from TGN46, and this segregation became clearer when VSVG began to leave the TGN (supplementary material Fig. S5).

We further visualized the mannose-6-phosphate receptors (MPRs) in starvation-induced autophagy. In cells co-transfected with CFP–CI-MRP and Cherry–LC3, during the entire process of starvation, MRP rarely targeted to the LC3-positive vesicles (Fig. 6B).

Taken together, these results confirmed that the LC3-posive vesicles budded from the TGN contain neither the constitutive cargo nor the components of TGN-to-endosome traffic.

Knockdown of AP1, but not AP2, inhibits autophagy

Given that AP1 and clathrin were targeted to autophagosomes, we performed RNAi to identify the necessity for AP1 and clathrin in autophagosome formation, with siRNA against AP2 as a control. The efficacy of the designed siRNA was confirmed by western blot (Fig. 7A). The effect of the siRNA treatment was assessed first by immunostaining. Compared with the control cells in which γ-adaptin or clathrin heavy-chain presented normal expression and peri-nuclear localization, knockdown cells displayed much fainter staining and a lack of TGN association and the number of starvation-induced LC3-positive autophagosomes was dramatically reduced (Fig. 7B,C). Data from western blots confirmed that knockdown of γ-adaptin or clathrin heavy-chain in HEK293 cells dramatically reduced the lipidated LC3-II levels triggered by starvation, with or without BafA1 treatment (Fig. 7D). Interestingly, the suppression of autophagosome number and LC3-II level was not detected in AP2-knockdown cells (Fig. 7B,C,D). These findings strongly suggest that AP1-mediated clathrin coating in the TGN but not AP2-mediated endocytosis plays a crucial role in starvation-induced autophagosome formation.

Discussion

The debate on the origin of the autophagosomal membrane and the formation of the autophagosome remains the most pivotal question for understanding autophagy. In this study, through our analysis of AP1-mediated events, we have shown that functional TGN membranes are required for autophagosome formation.

Our data showed how modulation of the secretory traffic modified the formation of autophagosomes in mammalian cells. By inactivation of the small GTPases that function in the early secretory pathway, we determined in animal cells the essential role of ER export in starvation-stimulated autophagy, which is consistent with the conclusion reached in yeast studies (Hamasaki et al., 2003; Ishihara et al., 2001). Nonetheless, owing to the close relationship between differential membrane trafficking routes, interruption of the early secretory pathway alters the late

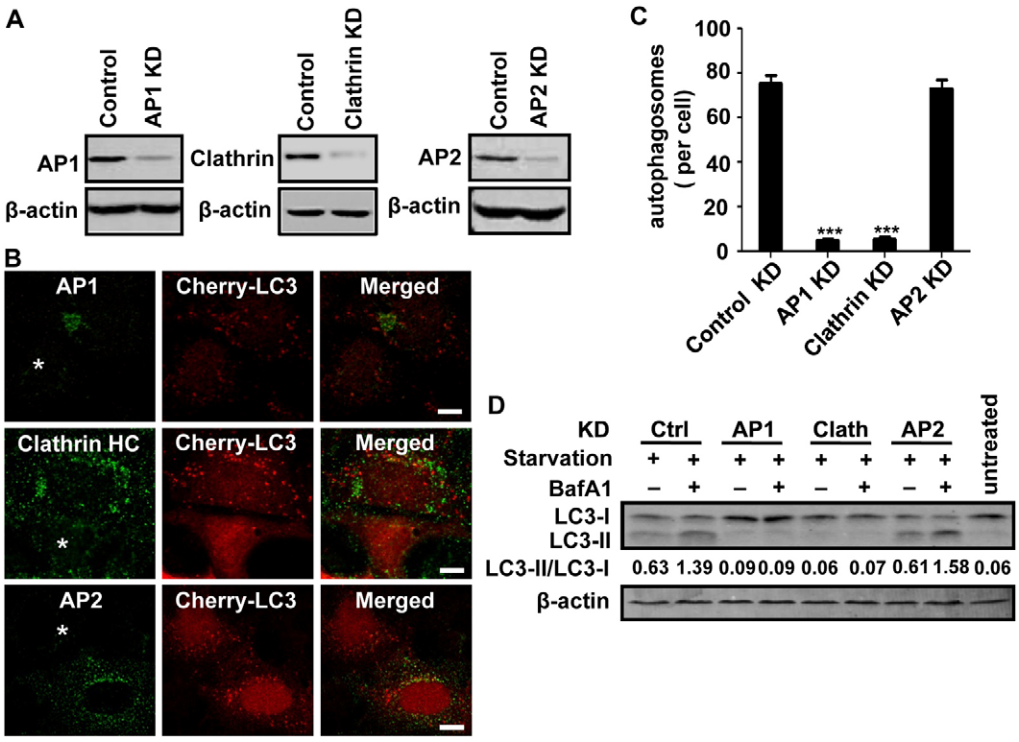

Fig. 7. Knockdown of AP1 inhibits starvation-induced autophagosome formation. (**A**) HEK293 cells were treated with siRNAs targeting to the AP1 γ-subunit, clathrin heavy-chain or AP2 α-subunit for 72 hours. Then the cells were analyzed by western blot to identify RNAi efficiency using specific antibodies against γ-adaptin, clathrin heavy chain or α-adaptin antibody. (**B**) HEK293 cells treated with AP1, clathrin heavy chain or AP2 siRNA for 48 hours. Then, the cells were transfected with Cherry–LC3. After 24 hours, the cells were starved for 1 hour, fixed and labeled with antibodies against γ-adaptin, clathrin heavy chain or α-adaptin. Gene-knockdown cells are indicated by asterisks. Scale bars: 10 μm. (**C**) Statistical analyses of the numbers of LC3 dots per cell in B. Quantification of autophagosomes was done by the Axiovision automatic measurement program on the Zeiss LSM510 Meta as described in the Materials and Methods. The values shown are means ± s.e.m.; ***$P<0.0001$ vs control cells. (**D**) HEK293 cells treated with siRNA against AP1, clathrin heavy chain or AP2 for 72 hours. Then the cells were cultured with starvation medium with or without BafA1 for 1 hour, and the cellular LC3 level was analyzed by western blot using LC3 antibody. The LC3-II to LC3-I ratio was evaluated by densitometric analysis.

transport to a great degree and breaks down the Golgi structure, which is central to intracellular trafficking. Observation of the time course of cargo flow and specific modulation of the TGN-to-PM traffic allowed us to determine that the post-Golgi transport regulated the process of autophagosome formation. Although surprising, it is not unreasonable to propose that a forced increase in the export of constitutively secreted proteins from the TGN stimulates the formation of autophagosomes. Many studies have suggested that lateral segregation in the TGN is the primary sorting event and that there is potential interdependence between the different domains (Gleeson et al., 2004; Hirschberg et al., 1998; Keller et al., 2001). In addition to the known necessity of AP1 and clathrin for TGN–endosome transport, the fact that dysfunction of AP1 and clathrin impeded VSVG transport to the PM supports the domain segregation model. Instead of functioning directly in the formation of TGN-to-PM carriers, AP1 and clathrin contribute to the constitutive cargo transport, possibly by facilitating the lateral segregation of the TGN membrane. Our results suggest the existence of specific discrete domains in the TGN membrane to which LC3 is recruited and from which the LC3-containing vesicles bud off. These specific domains are exclusive of the constitutive cargos and components destined for the endosomes; the formation and subsequent budding off of these domains are influenced by the post-Golgi traffic. This can explain not only the recent results from the yeast *Saccharomyces cerevisiae* showing that the post-Golgi Sec proteins and Golgi exit are required for autophagy (Geng et al., 2010; van der Vaart et al., 2010), but also an early report on animal cells demonstrating that post-Golgi but not ER or cis-Golgi membrane proteins are included in the limiting membranes of autophagosomes (Yamamoto et al., 1990). In addition, our results strongly imply that the formation of these LC3-positive vesicles is used by the cell to regulate intracellular membrane partitioning and redistribution.

Our finding showing the recruitment of LC3 to the TGN suggests that the TGN is not only a donor site for early LC3 assembly but also a membrane source for the formation of double-membrane autophagosomes. Instead of an accumulation of formed autophagic vesicles to the TGN, our observations indicate a direct association of LC3 with the TGN membrane in response to the presence of a mass of VSVG at the TGN or starvation-initiated signaling. During the time course of VSVG loading, very few LC3-containing vesicles were observed in the cytosol before VSVG arrived at the TGN, and LC3 vesicles were formed only when VSVG started to leave the TGN. Similarly, in starved cells, accumulation of LC3 in the peri-nuclear area occurred at a very early stage before LC3 vesicles were present in the cytosol. That the expression of AP180C or Eps15Δ95/295 blocked the formation of LC3 vesicles but not the VSVG-controlled association of LC3 with the TGN membrane further supports this conclusion. With regard to the membrane association of LC3, in vitro studies have pointed out the involvement of the orderly membrane recruitment of a series of Atg proteins, including the VPS34–beclin-1 and Atg5–Atg12–Atg16 complexes. Nevertheless, the precise role of these complexes and the underlying mechanism of LC3 binding, especially in mammalian cells, are still unclear. Our data suggest that a crucial step is the specific association of lipid-modified LC3 with TGN membranes. Possibly, during autophagy, upon association with the specific domain of the TGN, LC3 vesicles carry LC3 to the isolation membranes derived from the ER or other membrane compartments. During these processes, Atg9 plays an essential role in facilitating the docking of LC3–PE with the complexes, and AP1-mediated clathrin coating contributes to the budding off of LC3 vesicles from the TGN, although it is currently unknown whether the Atg5–Atg12–Atg16 complex exists in the TGN.

Our results are partially inconsistent with a recent report showing that knockdown of clathrin and AP2, but not AP1, inhibits the formation of autophagosomes (Ravikumar et al., 2010). However, the effect of knockdown of AP2 or epsin-1 on autophagosome formation appeared to be weak in the presence of BafA1, but not in samples without BafA1 treatment, and this has been interpreted as a possible decrease in LC3 II level in the absence of BafA1 and a low gene knockdown effect (Ravikumar et al., 2010). In our experimental system, even in the absence of BafA1, we showed clearly that knockdown of AP1 but not AP2 blocked starvation-initiated autophagosome formation. This was also confirmed by the effect of overexpression of the specific Eps15 mutant Eps15Δ14aa. Combined with the association of LC3 with the TGN and LC3 vesicles budding off the TGN, our observations support the conclusion that clathrin regulates the formation of autophagosomes by mainly functioning in the TGN but not the PM. We do not exclude a possible contribution of the PM to the autophagosome, at least in part because of the intimate membrane traffic between the TGN and the PM. To further clarify this issue, it will be especially crucial and interesting to find out whether the Atg16-positive and LC3-negative vesicles formed through clathrin–Atg16 interaction (Ravikumar et al., 2010) fuse with the TGN membrane (not the early or medial Golgi).

Materials and Methods

DNA constructs, reagents and antibodies

Arf1T31N–HA, Sar1T39N–HA, Sar1H79G–HA, VSVG–CFP, VSVG–Cherry, KDELR–GFP, YFP–Eps15Δ95/295 and CFP–TGN38 were described previously (Peters et al., 1995; Presley et al., 1997; Puertollano et al., 2001; Scales et al., 1997; Ward et al., 2001; Wu et al., 2003; Zaal et al., 1999). γ-adaptin–GFP, CFP–CI-MPR and AP180C–GFP were from Juan S. Bonifacino (National Institutes of Health, Bethesda, MD). Mito–YFP was from Clontech. GFP–α-adaptin was from Lois E. Greene (National Institutes of Health, Bethesda, MD). Eps15Δ14aa–Myc was kindly provided by Mark A. McNiven (Mayo Clinic College of Medicine, Rochester, MN). The cDNA of LC3 was a gift from Yoshinori Ohsumi (Tokyo Institute of Technology, Tokyo, Japan). GFP–LC3 was made by cloning the cDNA of LC3 into a PEGFP-C1 vector (Clontech Laboratories) using the *Bgl*II(5′) and *Sal*I (3′) restriction sites. Cherry–LC3 or YFP–LC3 were made by change the GFP in GFP–LC3 plasmid to mCherry or YFP, using the *Age*I and *Bsp*EI restriction sites. The point mutation for glycine to alanine at position 120 of LC3 (GFP–LC3G120A) was created by PCR-based site-directed mutagenesis using LC3 sense primer (5′-GCCTCCCAGGAGACGTTCGCGACAGCACTGGCTGTTACATAC-3′) and LC3 antisense primer (5′-GTATGTAACAGCCAGTGCTGTCGCGAACGTC-TCCTGGGAGGC-3′). Cherry–Atg9 was made by cloning the human autophagy 9-like 1 protein ORF (GenBank: BK004018.1) into a pmCherry-C1 vector (Clontech) using the *Eco*RI (5′) and *Xba*I (3′) restriction sites. Rapamycin and BafA1 were purchased from Sigma and used at 100 nM.

The following antibodies were used: rabbit polyclonal antibody against LC3 and mouse monoclonal antibody against β-actin (Sigma); mouse monoclonal antibodies against γ-adaptin (a subunit of AP1), α-adaptin (a subunit of AP2) and GFP (BD Biosciences); sheep polyclonal antibody against TGN46 (AbD Serotec); mouse monoclonal antibody against Myc and HA (Santa Cruz); mouse monoclonal antibody clathrin heavy chain (Cell Signaling). Alexa-Fluor-488- and Alexa-Fluor-545-tagged second antibodies were from Molecular Probes. Secondary antibodies goat anti-rabbit IRDye 800CW and goat anti-mouse IRDye 680 were from LI-COR Biosciences.

Cell culture and transfection

HEK293 cells were grown in DMEM supplemented with 10% FBS, 2 mM glutamine, 100 U/ml penicillin and 100 U/ml streptomycin, at 37℃ under 5% CO_2. Transient transfections were performed using Lipofectamine 2000 according

to the manufacturer's instructions (Invitrogen). Cells were analyzed 18–24 hours after transfection.

For the VSVG transport experiments, HEK293 cells growing on sterile glass coverslips were transfected with VSVG–Cherry using Lipofectamine 2000, then the cells were incubated at 40℃ overnight to maintain VSVG–Cherry in the ER. On the next day, cells were either kept at 40℃ or shifted to 32℃ for the indicated time. In some experiments, the cells were first shifted from 40℃ to 20℃ for 2 hours to accumulate VSVG–Cherry in the TGN, and then they were shifted to 32℃ for the indicated time.

For RNA interference, siRNA duplexes designed against conserved targeting sequences were transfected into HEK293 cells using Lipofectamine 2000 as specified by the manufacturer. The following siRNA duplexes were used: AAACCGAAUUAAGAAAGUGGUTT for γ-adaptin; GAGCAUGUGCACGC-UGGCCA for α-adaptin; AAGACCAAUUUCAGCAGACAGTT for clathrin heavy chain; AAGACCAAUUUCAGCAGACAGTT for control siRNA. All the siRNA duplexes were from GenePharma (Shanghai, China).

Autophagy induction by cell starvation or rapamycin treatment

To starve cells, they were washed three times with pre-warmed PBS then incubated in starvation medium (1% BSA, 140 mM NaCl, 1 mM $CaCl_2$, 1 mM $MgCl_2$, 5 mM glucose and 20 mM HEPES, pH 7.4) at 37℃ for the indicated times. In rapamycin-induced autophagy, cells were treated with 100 nM rapamycin.

Immunofluorescence staining and fluorescence microscopy

For immunostaining, HEK293 cells were fixed in 2% formaldehyde. After washing twice in PBS, cells were incubated in PBS with FBS (PBS, pH 7.4, 10% FBS) to block nonspecific sites of antibody adsorption. The cells were then incubated with appropriate primary and secondary antibodies in 0.1% saponin (Sigma) as indicated in the legends.

Images were taken in multitracking mode on a Zeiss LSM510 Meta laser-scanning confocal microscope (Carl Zeiss, Thornwood, NY) with a 63× Plan Apochromat 1.4 NA objective. Live-cell imaging was performed in LabTek chambers (Nalge Nunc International) which were maintained at 37℃ with 5% CO_2. In some experiments, a series of images through the *Z*-axis of the cell were taken and the stacks of images were reconstructed to create 3D images.

For quantification of the number of autophagosomes, a total of 50 cells were recorded and analyzed using the Axiovision Automatic measurement program on the Zeiss LSM510 Meta. LC3 punctae with a diameter between 0.3 and 1 μm were scored as positive.

Western blotting

Western blotting was performed as described previously (Liu et al., 1999). In brief, sample aliquots (40 μL) of proteins obtained from lysed cells were denatured and loaded on sodium dodecyl sulfate polyacrylamide gels. Afterwards, the proteins were transferred to PVDF membrane and subjected to western blotting. Membranes were blocked in TBST (150 mM NaCl, 10 mM Tris-HCl, pH 7.5 and 0.1% Tween 20) containing 5% (w/v) bovine serum albumin or milk, then incubated with the corresponding primary and secondary antibodies. The specific bands were analyzed using an Odyssey infrared imaging system (LI-COR Biosciences) after incubated with the corresponding secondary antibodies, goat anti-rabbit IRDye 800CW and goat anti-mouse IRDye 680 (LI-COR Biosciences, Lincoln, NE).

Acknowledgements

We thank Qiang Song and Yinggang Yan for technical support.

Funding

This study was supported by the National Basic Research Program of China [grant number 2011CB910100]; the Chinese 973 project [grant number 2010CB912103]; and the National Natural Science Foundation of China [grant numbers 30971429 and 31171288].

Supplementary material available online at
http://jcs.biologists.org/lookup/suppl/doi:10.1242/jcs.093203/-/DC1

References

Aridor, M., Bannykh, S. I., Rowe, T. and Balch, W. E. (1995). Sequential coupling between COPII and COPI vesicle coats in endoplasmic reticulum to Golgi transport. *J. Cell Biol.* **131**, 875-893.

Arstila, A. U. and Trump, B. F. (1968). Studies on cellular autophagocytosis. The formation of autophagic vacuoles in the liver after glucagon administration. *Am. J. Pathol.* **53**, 687-733.

Axe, E. L., Walker, S. A., Manifava, M., Chandra, P., Roderick, H. L., Habermann, A., Griffiths, G. and Ktistakis, N. T. (2008). Autophagosome formation from membrane compartments enriched in phosphatidylinositol 3-phosphate and dynamically connected to the endoplasmic reticulum. *J. Cell Biol.* **182**, 685-701.

Barlowe, C., Orci, L., Yeung, T., Hosobuchi, M., Hamamoto, S., Salama, N., Rexach, M. F., Ravazzola, M., Amherdt, M. and Schekman, R. (1994). COPII: a membrane coat formed by Sec proteins that drive vesicle budding from the endoplasmic reticulum. *Cell* **77**, 895-907.

Benmerah, A., Lamaze, C., Begue, B., Schmid, S. L., Dautry-Varsat, A. and Cerf-Bensussan, N. (1998). AP-2/Eps15 interaction is required for receptor-mediated endocytosis. *J. Cell Biol.* **140**, 1055-1062.

Bergmann, J. E. (1989). Using temperature-sensitive mutants of VSV to study membrane protein biogenesis. *Methods Cell Biol.* **32**, 85-110.

Chi, S., Cao, H., Chen, J. and McNiven, M. A. (2008). Eps15 mediates vesicle trafficking from the trans-Golgi network via an interaction with the clathrin adaptor AP-1. *Mol. Biol. Cell* **19**, 3564-3575.

Darke, K. R., Kang, M. and Kenworthy, A. K. (2010). Nucleocytoplasmic distribution and dynamics of the autophagosome marker EGFP-LC3. *PLoS ONE* **5**, e9806.

Dascher, C. and Balch, W. E. (1994). Dominant inhibitory mutants of ARF1 block endoplasmic reticulum to Golgi transport and trigger disassembly of the Golgi apparatus. *J. Biol. Chem.* **269**, 1437-1448.

Ericsson, J. L. (1969). Studies on induced cellular autophagy. II. Characterization of the membranes bordering autophagosomes in parenchymal liver cells. *Exp. Cell Res.* **56**, 393-405.

Ford, M. G., Pearse, B. M., Higgins, M. K., Vallis, Y., Owen, D. J., Gibson, A., Hopkins, C. R., Evans, P. R. and McMahon, H. T. (2001). Simultaneous binding of PtdIns(4,5)P2 and clathrin by AP180 in the nucleation of clathrin lattices on membranes. *Science* **291**, 1051-1055.

Geng, J., Nair, U., Yasumura-Yorimitsu, K. and Klionsky, D. J. (2010). Post-golgi sec proteins are required for autophagy in Saccharomyces cerevisiae. *Mol. Biol. Cell* **21**, 2257-2269.

Gleeson, P. A., Lock, J. G., Luke, M. R. and Stow, J. L. (2004). Domains of the TGN: coats, tethers and G proteins. *Traffic* **5**, 315-326.

Griffiths, G., Pfeiffer, S., Simons, K. and Matlin, K. (1985). Exit of newly synthesized membrane proteins from the trans cisterna of the Golgi complex to the plasma membrane. *J. Cell Biol.* **101**, 949-964.

Hailey, D. W., Rambold, A. S., Satpute-Krishnan, P., Mitra, K., Sougrat, R., Kim, P. K. and Lippincott-Schwartz, J. (2010). Mitochondria supply membranes for autophagosome biogenesis during starvation. *Cell* **141**, 656-667.

Hamasaki, M., Noda, T. and Ohsumi, Y. (2003). The early secretory pathway contributes to autophagy in yeast. *Cell Struct. Funct.* **28**, 49-54.

Hayashi-Nishino, M., Fujita, N., Noda, T., Yamaguchi, A., Yoshimori, T. and Yamamoto, A. (2009). A subdomain of the endoplasmic reticulum forms a cradle for autophagosome formation. *Nat. Cell Biol.* **11**, 1433-1437.

Hirschberg, K., Miller, C. M., Ellenberg, J., Presley, J. F., Siggia, E. D., Phair, R. D. and Lippincott-Schwartz, J. (1998). Kinetic analysis of secretory protein traffic and characterization of Golgi to plasma membrane transport intermediates in living cells. *J. Cell Biol.* **143**, 1485-1503.

Ishihara, N., Hamasaki, M., Yokota, S., Suzuki, K., Kamada, Y., Kihara, A., Yoshimori, T., Noda, T. and Ohsumi, Y. (2001). Autophagosome requires specific early Sec proteins for its formation and NSF/SNARE for vacuolar fusion. *Mol. Biol. Cell* **12**, 3690-3702.

Itoh, T., Fujita, N., Kanno, E., Yamamoto, A., Yoshimori, T. and Fukuda, M. (2008). Golgi-resident small GTPase Rab33B interacts with Atg16L and modulates autophagosome formation. *Mol. Biol. Cell* **19**, 2916-2925.

Juhasz, G. and Neufeld, T. P. (2006). Autophagy: a forty-year search for a missing membrane source. *PLoS Biol.* **4**, e36.

Kabeya, Y., Mizushima, N., Ueno, T., Yamamoto, A., Kirisako, T., Noda, T., Kominami, E., Ohsumi, Y. and Yoshimori, T. (2000). LC3, a mammalian homologue of yeast Apg8p, is localized in autophagosome membranes after processing. *EMBO J.* **19**, 5720-5728.

Keller, P., Toomre, D., Diaz, E., White, J. and Simons, K. (2001). Multicolour imaging of post-Golgi sorting and trafficking in live cells. *Nat. Cell Biol.* **3**, 140-149.

Kihara, A., Kabeya, Y., Ohsumi, Y. and Yoshimori, T. (2001). Beclin-phosphatidylinositol 3-kinase complex functions at the trans-Golgi network. *EMBO Rep.* **2**, 330-335.

Klausner, R. D., Donaldson, J. G. and Lippincott-Schwartz, J. (1992). Brefeldin A: insights into the control of membrane traffic and organelle structure. *J. Cell Biol.* **116**, 1071-1080.

Kuge, O., Dascher, C., Orci, L., Rowe, T., Amherdt, M., Plutner, H., Ravazzola, M., Tanigawa, G., Rothman, J. E. and Balch, W. E. (1994). Sar1 promotes vesicle budding from the endoplasmic reticulum but not Golgi compartments. *J. Cell Biol.* **125**, 51-65.

Liu, W., Akhand, A. A., Kato, M., Yokoyama, I., Miyata, T., Kurokawa, K., Uchida, K. and Nakashima, I. (1999). 4-hydroxynonenal triggers an epidermal growth factor receptor-linked signal pathway for growth inhibition. *J. Cell Sci.* **112**, 2409-2417.

Lui-Roberts, W. W., Collinson, L. M., Hewlett, L. J., Michaux, G. and Cutler, D. F. (2005). An AP-1/clathrin coat plays a novel and essential role in forming the Weibel-Palade bodies of endothelial cells. *J. Cell Biol.* **170**, 627-636.

Matlin, K. S. and Simons, K. (1983). Reduced temperature prevents transfer of a membrane glycoprotein to the cell surface but does not prevent terminal glycosylation. *Cell* **34**, 233-243.

Peters, P. J., Hsu, V. W., Ooi, C. E., Finazzi, D., Teal, S. B., Oorschot, V., Donaldson, J. G. and Klausner, R. D. (1995). Overexpression of wild-type and

mutant ARF1 and ARF6: distinct perturbations of nonoverlapping membrane compartments. *J. Cell Biol.* **128**, 1003-1017.

Presley, J. F., Cole, N. B., Schroer, T. A., Hirschberg, K., Zaal, K. J. and Lippincott-Schwartz, J. (1997). ER-to-Golgi transport visualized in living cells. *Nature* **389**, 81-85.

Pucadyil, T. J. and Schmid, S. L. (2009). Conserved functions of membrane active GTPases in coated vesicle formation. *Science* **325**, 1217-1220.

Puertollano, R., Aguilar, R. C., Gorshkova, I., Crouch, R. J. and Bonifacino, J. S. (2001). Sorting of mannose 6-phosphate receptors mediated by the GGAs. *Science* **292**, 1712-1716.

Ravikumar, B., Moreau, K., Jahreiss, L., Puri, C. and Rubinsztein, D. C. (2010). Plasma membrane contributes to the formation of pre-autophagosomal structures. *Nat. Cell Biol.* **12**, 747-757.

Reggiori, F. and Tooze, S. A. (2009). The EmERgence of autophagosomes. *Dev. Cell* **17**, 747-748.

Reggiori, F., Wang, C. W., Nair, U., Shintani, T., Abeliovich, H. and Klionsky, D. J. (2004). Early stages of the secretory pathway, but not endosomes, are required for Cvt vesicle and autophagosome assembly in Saccharomyces cerevisiae. *Mol. Biol. Cell* **15**, 2189-2204.

Reggiori, F., Shintani, T., Nair, U. and Klionsky, D. J. (2005). Atg9 cycles between mitochondria and the pre-autophagosomal structure in yeasts. *Autophagy* **1**, 101-109.

Scales, S. J., Pepperkok, R. and Kreis, T. E. (1997). Visualization of ER-to-Golgi transport in living cells reveals a sequential mode of action for COPII and COPI. *Cell* **90**, 1137-1148.

Shima, D. T., Cabrera-Poch, N., Pepperkok, R. and Warren, G. (1998). An ordered inheritance strategy for the Golgi apparatus: visualization of mitotic disassembly reveals a role for the mitotic spindle. *J. Cell Biol.* **141**, 955-966.

Sou, Y. S., Tanida, I., Komatsu, M., Ueno, T. and Kominami, E. (2006). Phosphatidylserine in addition to phosphatidylethanolamine is an in vitro target of the mammalian Atg8 modifiers, LC3, GABARAP, and GATE-16. *J. Biol. Chem.* **281**, 3017-3024.

Tanida, I., Ueno, T. and Kominama, E. (2004). LC3 conjugation system in mammalian autophagy. *Int. J. Biochem. Cell Biol.* **36**, 2503-2518.

van der Vaart, A., Griffith, J. and Reggiori, F. (2010). Exit from the golgi is required for the expansion of the autophagosomal phagophore in yeast Saccharomyces cerevisiae. *Mol. Biol. Cell* **21**, 2270-2284.

Ward, T. H., Polishchuk, R. S., Caplan, S., Hirschberg, K. and Lippincott-Schwartz, J. (2001). Maintenance of Golgi structure and function depends on the integrity of ER export. *J. Cell Biol.* **155**, 557-570.

Wu, X., Zhao, X., Puertollano, R., Bonifacino, J. S., Eisenberg, E. and Greene, L. E. (2003). Adaptor and clathrin exchange at the plasma membrane and trans-Golgi network. *Mol. Biol. Cell* **14**, 516-528.

Yamamoto, A., Masaki, R. and Tashiro, Y. (1990). Characterization of the isolation membranes and the limiting membranes of autophagosomes in rat hepatocytes by lectin cytochemistry. *J. Histochem. Cytochem.* **38**, 573-580.

Yen, W. L., Shintani, T., Nair, U., Cao, Y., Richardson, B. C., Li, Z., Hughson, F. M., Baba, M. and Klionsky, D. J. (2010). The conserved oligomeric Golgi complex is involved in double-membrane vesicle formation during autophagy. *J. Cell Biol.* **188**, 101-114.

Yla-Anttila, P., Vihinen, H., Jokitalo, E. and Eskelinen, E. L. (2009). 3D tomography reveals connections between the phagophore and endoplasmic reticulum. *Autophagy* **5**, 1180-1185.

Young, A. R., Chan, E. Y., Hu, X. W., Kochl, R., Crawshaw, S. G., High, S., Hailey, D. W., Lippincott-Schwartz, J. and Tooze, S. A. (2006). Starvation and ULK1-dependent cycling of mammalian Atg9 between the TGN and endosomes. *J. Cell Sci.* **119**, 3888-3900.

Zaal, K. J., Smith, C. L., Polishchuk, R. S., Altan, N., Cole, N. B., Ellenberg, J., Hirschberg, K., Presley, J. F., Roberts, T. H., Siggia, E. et al. (1999). Golgi membranes are absorbed into and reemerge from the ER during mitosis. *Cell* **99**, 589-601.

Zhao, X., Greener, T., Al-Hasani, H., Cushman, S. W., Eisenberg, E. and Greene, L. E. (2001). Expression of auxilin or AP180 inhibits endocytosis by mislocalizing clathrin: evidence for formation of nascent pits containing AP1 or AP2 but not clathrin. *J. Cell Sci.* **114**, 353-365.

Journal of Cell Science